Small acoustic tubes: New approximations including isothermal and viscous effects[a)]

Joseph C. Zuercher,[b)] Elmer V. Carlson, and Mead C. Killion[c)]
Industrial Research Products, Inc., Elk Grove Village, Illinois 60007

(Received 19 December 1986; accepted for publication 4 January 1988)

Algebraic expressions are given (in FORTRAN format for convenient use) that accurately approximate the value of the per unit-length acoustic impedance of small tubes (radii less than $\frac{1}{16}$ acoustic wavelength) including isothermal and viscous effects. Their accuracy of typically 3% or better was obtained as a result of adding a shunt conductance term to the traditional approximations and including frequency-dependent multiplicative factors. The multiplicative factors are simple expressions for the real or imaginary terms, providing a factor of 40 increase in calculational speed over the full Bessel-function solution. Experimental verification is presented for various combinations of small tubes and cavities relevant to hearing aid applications, and the differences between the present approximations and previous approximations are illustrated using a 1-mm-diam tube as an example. Normalized complex series impedance and shunt admittance, characteristic impedance, time delay, and attenuation constant plots are provided as a reference utilizing the more nearly exact Bessel solution.

PACS numbers: 43.85.Bh, 43.20.Mv

INTRODUCTION

A. Background

If an acoustic tube is connected between a source of pressure $P1$ and an acoustic load (which may be another tube) of complex acoustic input impedance $Z2$, it will present to the source an input impedance of $Z1$ and produce a (complex) pressure $P2$ across the load (see Fig. 1). The relationships between these quantities are given by the transmission line equations (see, e.g., Flanagan[1]), which can be expressed as

$$\frac{Z1}{Z0}=\frac{Z2*\mathrm{COSH(LENGTH*GAMMA)}+Z0*\mathrm{SINH(LENGTH*GAMMA)}}{Z0*\mathrm{COSH(LENGTH*GAMMA)}+Z2*\mathrm{SINH(LENGTH*GAMMA)}}, \tag{1}$$

$$P1/P2=\mathrm{COSH(LENGTH*GAMMA)}+(Z0/Z2)*\mathrm{SINH(LENGTH*GAMMA)}, \tag{2}$$

where LENGTH is the length of the tube, $Z0$ is its characteristic impedance, and GAMMA is its complex propagation constant. (Here and throughout the text, we will use spelled-out symbols and designate multiplication by "*" and exponentiation by "**," following the conventions of popular computer languages such as FORTRAN.[2] RADIUS is denoted by "a" in the figures themselves, however.)

The characteristic impedance $Z0$, and propagation constant GAMMA, of a small tube can be expressed in terms of the series impedance per unit-length ZT and the shunt admittance per unit-length YT of the tube

$$Z0=\mathrm{SQRT}(ZT/YT), \tag{3}$$

$$\mathrm{GAMMA}=\mathrm{SQRT}(ZT*YT). \tag{4}$$

The exact solution for the complex quantities ZT and YT (in cgs acoustical ohms and mhos, respectively) was given more than a century ago by Helmholtz[3] and Kirchhoff,[4] and more recently for the low-frequency case by Iberall[5] and Zwikker and Kosten,[6] but involves the calculation of a sufficient number of terms in the integral representation of the complex Bessel functions $J0$ and $J1$ to insure sufficient accuracy in the answer, a tedious process at best. For this reason, approximations to the exact solution have been commonly used for engineering purposes. Olson[7] (pp. 89 and 91), for example, gives the following approximations (given here on a per unit-length basis):

$$ZT=[1/\mathrm{AREA}]*[8*U/\mathrm{RADIUS}**2 + J*(4/3)*W*\mathrm{RHO}], \tag{5}$$

$$YT=J*W*\mathrm{AREA}/(\mathrm{RHO}*C**2), \tag{6}$$

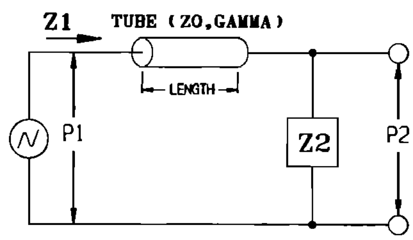

FIG. 1. Definition of input (1) and output (2) impedance and pressure for an acoustic tube treated as a transmission line.

[a)] Originally presented December 1977 at the 94th Meeting of the Acoustical Society of America, Miami Beach, FL [J. Acoust. Soc. Am. Suppl. 1 62, S56 (1977)].
[b)] Present address: Eaton Corp., Milwaukee, WI 53216.
[c)] Present address: Etymotic Research, Elk Grove Village, IL 60007.

 0001-4966/88/041653-08$00.80

where the RADIUS and cross-sectional AREA of the tube are given in cm and cm^2, respectively, the angular frequency $W = 2*PI*FREQ$, the complex unit $J = SQRT(-1)$, and U, RHO, and C are the viscosity, density, and speed of sound of air, respectively.

While the traditional approximations such as (5) and (6) are often adequate, in certain frequency ranges they can produce relatively large errors: up to 40% in compliance, 33% in inertance, and even larger discrepancies in resistance. [Indeed, the shunt conductance term, which can amount to 10% or more of the shunt admittance in the isothermal–adiabatic transition region, is ignored entirely in (6).]

Flanagan[1] derived algebraic approximations, treating the shunt conductance term separately, in better agreement with the full Bessel-function solutions. Flanagan was primarily interested in vocal-tract-size tubes, however, and assumed adiabatic conditions for the volume compliance at all frequencies and used a series resistance approximation that goes toward zero at low (in the case of vocal-tract-size tubes, subaudible) frequencies. For the smaller tubes of primary interest to us, the increased volume compliance in the adiabatic-to-isothermal transition region is often of critical importance, and the actual series resistance (which does not tend toward zero but becomes constant at low frequencies) is often an important part of the total impedance.

Most recently, Keefe[8] has provided separate algebraic approximations for small and large diameter tubes with an improvement to less than 10% error in the overlapping transition region. Unfortunately, in the case of the hearing aid tubes of primary interest to us, that transition region often occurs at frequencies where the performance of the hearing aid is of most interest.

The main purpose of this article is to describe improved approximations for the series impedance per unit-length ZT and the shunt admittance per unit-length YT of small acoustic tubes, specifically including those important to hearing aid applications. Discrepancies in using the new approximations compared to the Bessel theory are usually less than 3% at any frequency for which the radius is less than $\frac{1}{16}$ of a wavelength, except in the case of the shunt conductance term, where larger discrepancies occur at frequencies remote from the isothermal-to-adiabatic transition region. In the latter case, however, the discrepancy in phase angle of the shunt admittance (compliance and conductance) is held within less than 1° of the Bessel theory.

B. The new approximation

The new approximations are

$$ZT = [1/\text{AREA}]*[(8*U/\text{RADIUS}**2)*M1 + J*W*\text{RHO}*M2], \quad (7)$$

$$YT = [\text{AREA}/(\text{RHO}*C**2)] *[(1/\text{RADIUS}**2)*M3 + J*W*M4]. \quad (8)$$

The dimensionless multipliers $M1$–$M4$ used in Eqs. (7) and (8) are given in closed form by the algebraic expressions

$$M1 = [\text{SQRT}(1 + 0.214*WN)]/[1 + 0.24 *WN/(2.2 + WN**2) - 2.2*WN/(625 + WN**2)], \quad (9)$$

$$M2 = \text{SQRT}[(1.69 + 0.05*WN)/(1 + 0.05*WN)], \quad (10)$$

$$M3 = 0.303*WN**2/\{(1 + 0.3*WN**1.6)**0.33 *[1 + WN**2/(1 + 0.3*WN**1.6)**0.66]\}, \quad (11)$$

$$M4 = 1 + 0.4/\{1 + [WN/(0.61 + 0.79*WN**0.75)]**2\}, \quad (12)$$

where $WN = W*\text{RADIUS}**2$ is taken as a normalized angular frequency[9] when calculating the values for $M1$–$M4$. Note that the traditional approximations given in (5) and (6) can be obtained from Eqs. (7) and (8) by setting $M1 = M4 = 1$, $M2 = 4/3$, and $M3 = 0$.

C. Evolution of the new approximations

The form of Eq. (8) for the shunt admittance per unit-length was chosen based on the similarity of the calculated admittance (see Fig. 8) with that of a simple R–C circuit. Such a simple approximation has been used before to represent isothermal effects (Hueter and Bolt[10]).

An initial approximation for the shunt admittance was obtained directly from multisection R–C networks by manual curve fitting. Unfortunately, this method invariably led to lumpy fits. A major refinement came when slowly changing functions were constructed from algebraic expressions using fractional exponents (note the equations for $M3$ and $M4$) to define a frequency mapping to transform the network response so that it matched the Bessel response (shown later in Fig. 8). Encouraged by this success using simple algebraic expressions, the series mass reactance factor was approximated with an expression ($M2$) involving a square root of the ratio of two first-order polynomials. The series resistance factor ($M1$) required more complicated polynomials, arrived at in an intuitive fashion after intuition had been trained by observation, comparing (computer plots of) many trial expressions to the Bessel solution.

Benade[11] had previously given an improved set of approximations in the form of asymptotic equations, but a table of "look-up" values (provided) was required to cover the important transition region between asymptotes. Thus the present approximations can also be considered as an extension of Benade's work with Eqs. (9)–(11) providing the functional equivalent of his look-up table.

The time to calculate expressions (7)–(12) on a Honeywell 1648 digital computer using FORTRAN IV is about 0.024 s, compared to 1.0 s to calculate sufficient terms in the Bessel-function solutions to evaluate the same quantities to the same accuracy, an increase in computational speed of about 40 times. (These benchmarks were performed in 1976, when the 1648 was a popular time-sharing mainframe computer.) Even a pocket calculator such as the hp 41CV can calculate expressions (7)–(12) in roughly 15 s. One of the reasons for this improved computational efficiency is the fact that $M1$–$M4$ are calculated using real-number arithmetic. For the above time comparisons, the computationally efficient Bessel's integral representation[12] as given in Eq. (18), below, was used to evaluate the Bessel functions in the complex domain. A truncated infinite series representation would have required even more computer time. (Using an infinite series would have taken forever, of course.)

D. Relevance to traditional approximations

Figure 2 illustrates the region of applicability of the new approximations in comparison to previous approximations. The low-frequency values for tube resistance and inertance as quoted by Olson[7] were based on Poissell's equation (Lamb[13]) and the definition of inertia. This is shown as model (a) in Fig. 2. A common "high"-frequency approximation is shown in Fig. 1(b) representing Morse and Ingard's[14] calculations. Both can be compared with model (c) that represents the present approximations. The stated (frequency) ranges of applicability are also indicated in the figure. The transition frequency ($F = 0.16$/RADIUS**2) for the impedances in (c) lies outside the regions of applicability of either (a) or (b).

Golay[15] and Daniels[16] have found it expedient to consider the tube as an enclosure only (and not as a transmission line). Biagi and Cook[17] and Bruel[18] have been interested in the total magnitude of compliance. Crandall[19] was more concerned with transmission through a tube (viscoinertial effects). Although any of these simplifications can be justified for the specific application in mind, they do not simultaneously account for viscosity, inertia, compressibility, and the existence of an isothermal boundary over the entire frequency range from dc up to the frequency at which the RADIUS becomes $\frac{1}{16}$ of a wavelength, as does the present model (c). For example, neither (a) nor (b) explicitly accounts for the low-frequency increase in compliance due to isothermal effects. Model (b) lumps the isothermal and viscous losses into one series resistance, which adequately accounts for the damping in standing wave tube resonances; however, if the series inertance of the tube resonates with an external load compliance, only the viscous loss affects the actual response, so that model (b) provides too much damping.

I. EXPERIMENTAL DATA

The approximate model presented here has been successfully used (in essentially the present form) for well over a decade as part of a complete program for the modeling of hearing aid transducers, ear simulators, and other systems. In nearly all cases, the agreement between calculated and experimental results had been within the range of experimental error (see, for example, the comparisons shown by Carlson and Killion[20] obtained with an earlier approximation), but a careful comparison between the various models and experimental results was lacking. The following series of experiments was designed to fulfill that need. In most cases, the attenuation of sound transmitted through a tube terminated in a rigid cavity was measured.

A. Tube terminated in a cavity

Figure 3 shows the experimental setup used. The quantity measured was the ratio of the pressure developed at the microphone in the cavity ($P2$) to that at the tube entrance ($P1$), and is termed "ATTENUATION." A calibration curve was run on a miniature sensing microphone placed just in front of the reference microphone to establish the frequency dependence of its sensitivity. Various volumes were attached to a 5-cm tube of radius 0.079 cm. The computer predictions based on various models are shown, terminated in two different load volumes, along with the measured data (dashed) in Figs. 4 and 5. The first peak on each curve is primarily due to the resonance of the tube inertance with the cavity volume (a Helmholtz resonator); subsequent peaks are due to standing waves in the tube. As can be seen, too much damping and too little inertance are present in the high-frequency model (b) at the tube–cavity resonance. The

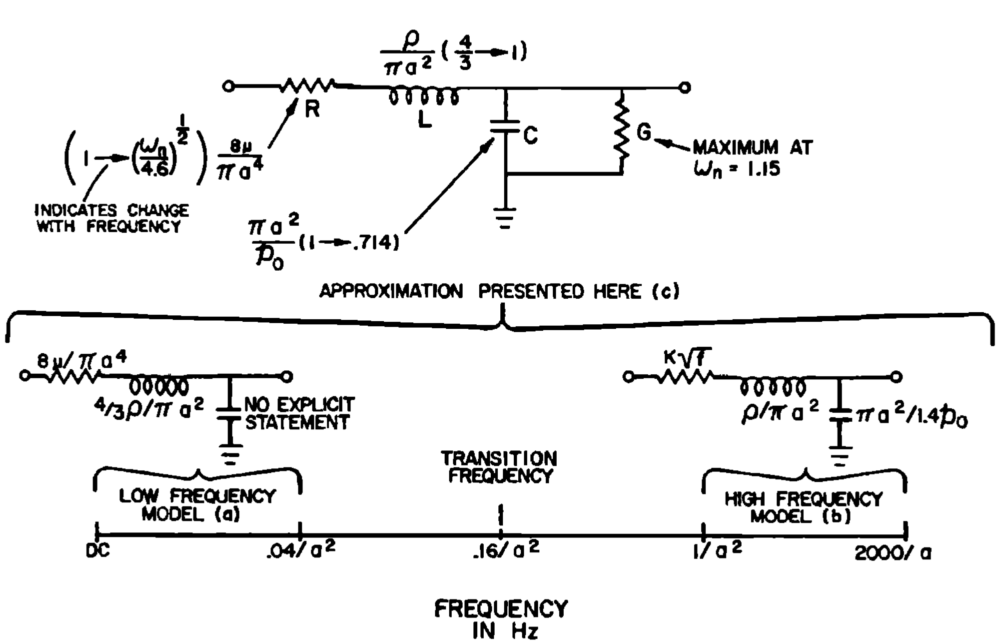

FIG. 2. Circuit representation of various models of per unit-length tube impedance, and stated ranges of applicability. The parenthetical term for each element gives the low- and high-frequency asymptotic values, with the arrow pointing to the high-frequency value. Region (a) refers to Lamb,[13] and (b) to Morse and Ingard.[14]

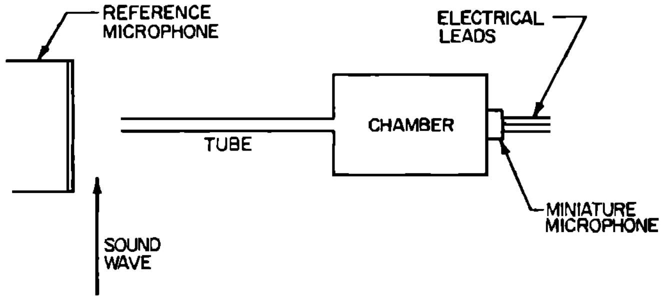

FIG. 3. Sketch of experimental setup used to measure response (pressure ratio $P2/P1$) of tube connected to a load volume.

low-frequency model (a) coincides with (c) in its limited range of applicability (below 6 kHz). Other data (not presented here) were taken on tubes of a variety of diameters and lengths that generally agreed with a computer prediction using the present model (c).

B. Tube terminated in a microphone

In this case, the miniature sensing microphone formed the entire load; i.e., a tube was attached directly to the inlet of a hearing aid type microphone. First, an analog equivalent circuit was determined that correctly described the microphone. This circuit was then added to the model for a 5-cm tube, with the results shown in Fig. 6. As in the previous examples, the high-frequency model (b), where it applies, predicts less inertance and more damping than the proposed approximation (c). Stewart and Lindsay[21] suggested an additional correction term for inertance that would extend the region of applicability of model (b) down to the transition frequency. However, no correction for loss was included.

Egolf[22] used a four-terminal network solution of a probe-tube microphone system incorporating a Bessel-function approximation for the tube impedance. Although his approach represented a general description of a tube, the particular probe-tube microphone system selected, because of the heavily damped resonance, did not show a material

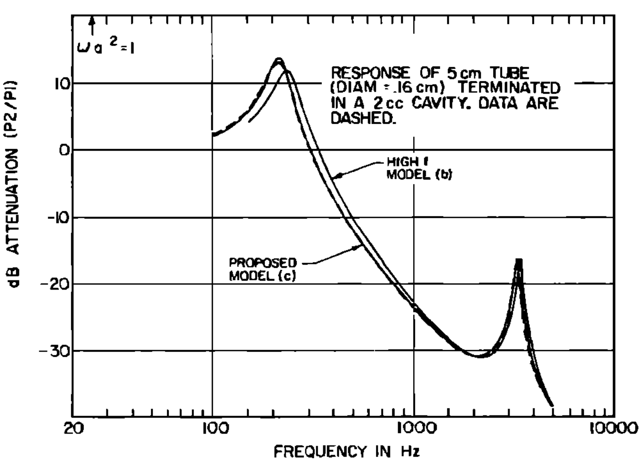

FIG. 4. Calculated response of 5-cm tube of 1.6-mm inner diameter ($a = 0.08$ cm) terminated in a 2-cm^3 cavity. Measured data are shown dashed.

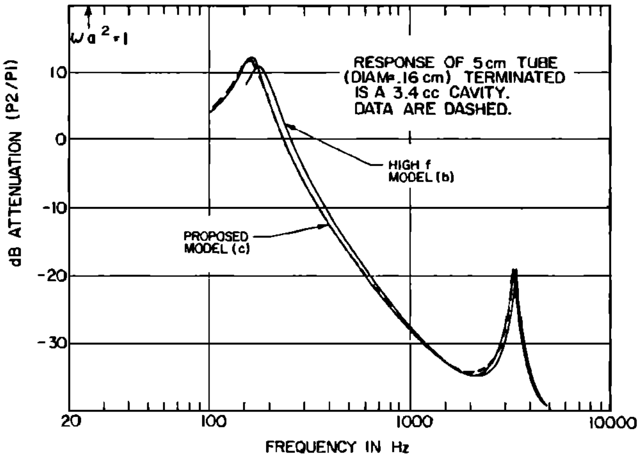

FIG. 5. Calculated response of same tube (5 cm of 1.6-mm diameter) terminated in a 3.4-cc cavity. Measured data are shown dashed.

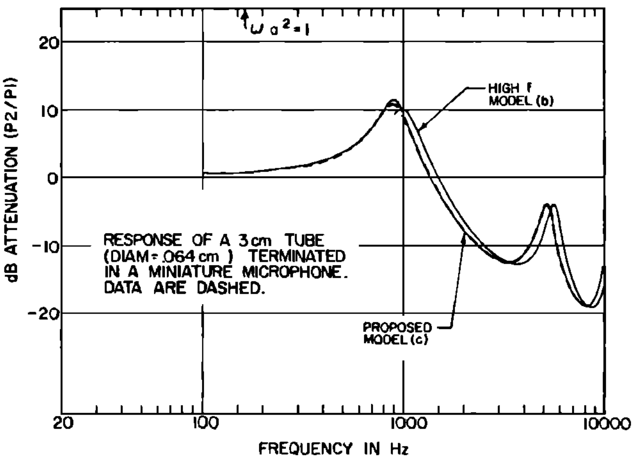

FIG. 6. Calculated response of a 3-cm tube of 0.64-mm inner diameter ($a = 0.032$ cm) terminated in a miniature microphone. Measured data are shown dashed.

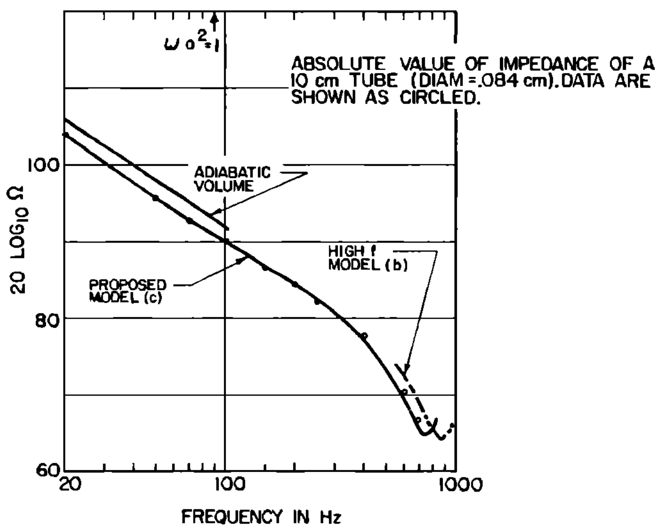

FIG. 7. Calculated impedance magnitude of a 10-cm tube of 0.84-mm inner diameter ($a = 0.042$ cm). Measured data are shown as circled.

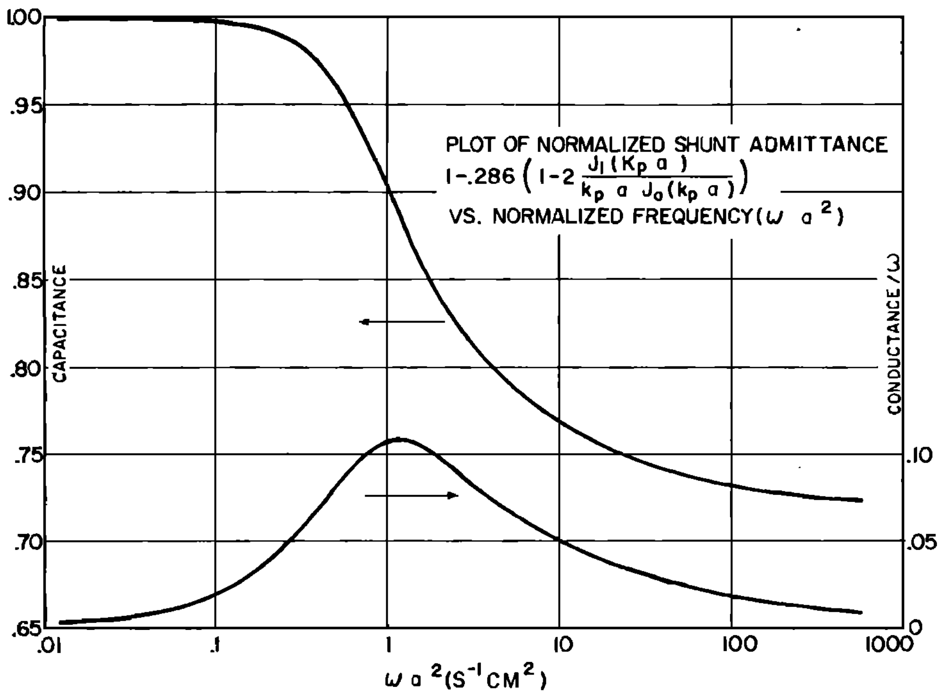

FIG. 8. Plot of normalized shunt admittance versus normalized frequency ($=\omega * a^2$) calculated using the full Bessel-function solution.

difference between the more exact Bessel approximation (c) and the high-frequency model (b).

C. Tube impedance data

In order to demonstrate the effect of a low-frequency compliance increase due to heat flow, the impedance of a tube was measured using a substitution method. The results are shown in Fig. 7. To acquire the experimental impedance data, the response of a blocked calibrated volume was compared to the response of the same volume with the acoustic tube attached. Corrections due to phase shift were applied to these data based on the effects of the first-tube resonance.

The entire frequency range is adequately described by the present model (c), removing the limitations in magnitude and range of the adiabatic model (a) or the high-frequency model (b).

II. DATA FROM THE EXACT BESSEL-FUNCTION SOLUTION

A. Tube theory development

A general review of tube theories and approximations is given by Tijdman.[23] Attention is restricted here to the case of small amplitude waves for which the acoustic wavelength is much larger than the tube radius. At 10 kHz, this limits tube diameters to less than about 4 mm (Beranek[24]). Moreover, it is assumed that molecular dissipation losses (in air about $2*10^{-4}$ Np/cm) are small compared to viscous and isothermal losses (Kinsler and Frey[25]).

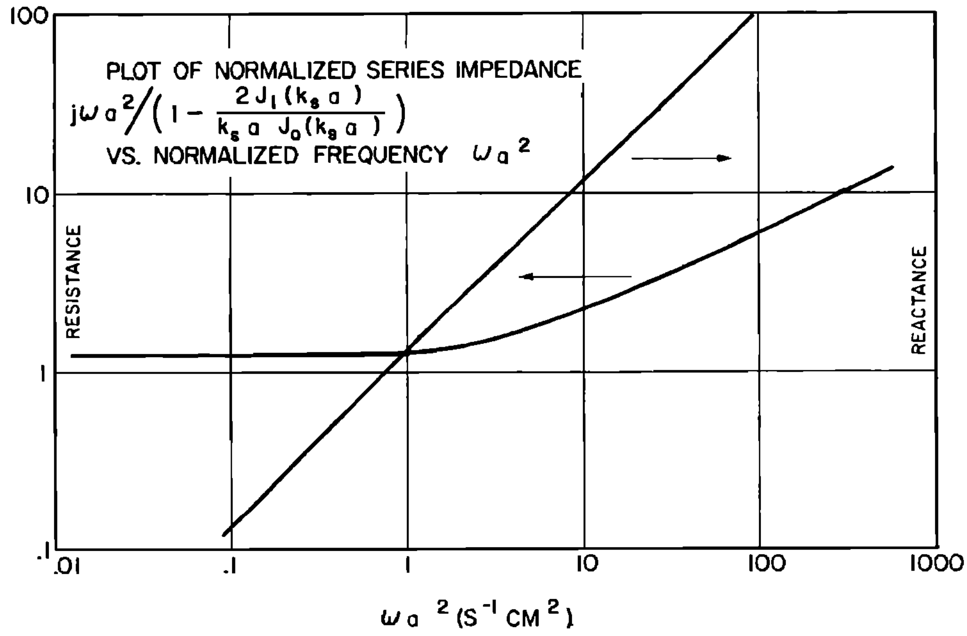

FIG. 9. Plot of normalized series impedance versus normalized frequency ($=\omega * a^2$) calculated using the full Bessel-function solution.

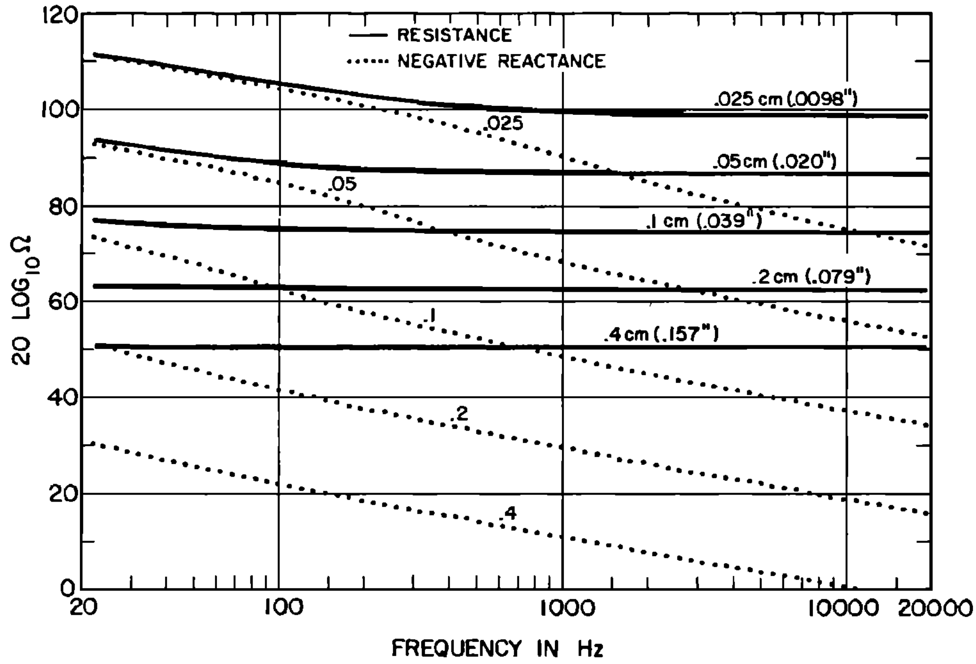

FIG. 10. Characteristic impedance of a circular tube with diameter as parameter calculated using the full Bessel-function solution.

The characteristic impedance of a tube depends solely on the tube per unit-length series impedance and shunt admittance. The series impedance was originally derived by Helmholtz,[3] who assumed a simple adiabatic volume in shunt. Kirchhoff[4] added isothermal effects to this model to properly explain other losses noted experimentally by Kundt.[26]

In the long-wave limit, the resulting equations are equivalent to those determined by Iberall[5] or Zwikker and Koston[6] in their low-reduced-frequency solutions, given here in a form similar to that used by Keefe[8]:

$$ZT = J*W*(\mathrm{RHO}/\mathrm{AREA})/ \{1-2*J1(KS*\mathrm{RADIUS})/ [KS*\mathrm{RADIUS}*J0(KS*\mathrm{RADIUS})]\}, \quad (13)$$

$$YT = J*W*(V0/P0)*(1-0.286 *\{1-2*J1(KP*\mathrm{RADIUS})/ [KP*\mathrm{RADIUS}*J0(KP*\mathrm{RADIUS})]\}), \quad (14)$$

where $J0$ and $J1$ are the zero- and first-order Bessel functions, $V0$ and $P0$ are the tube volume and atmospheric pressure, respectively, and KS and KP are the series and shunt wavenumbers given by

$$KS = \mathrm{SQRT}(-J*W*\mathrm{RHO}/U), \quad (15)$$

$$KP = \mathrm{SQRT}(-J*W/H**2), \quad (16)$$

where J, W, RHO, U, and RADIUS are as defined above with Eqs. (5) and (6), and $H**2$ is the thermal diffusivity of air approximated by

$$H**2 = \mathrm{KAPPA}/(\mathrm{RHO}*CP) \quad (17)$$

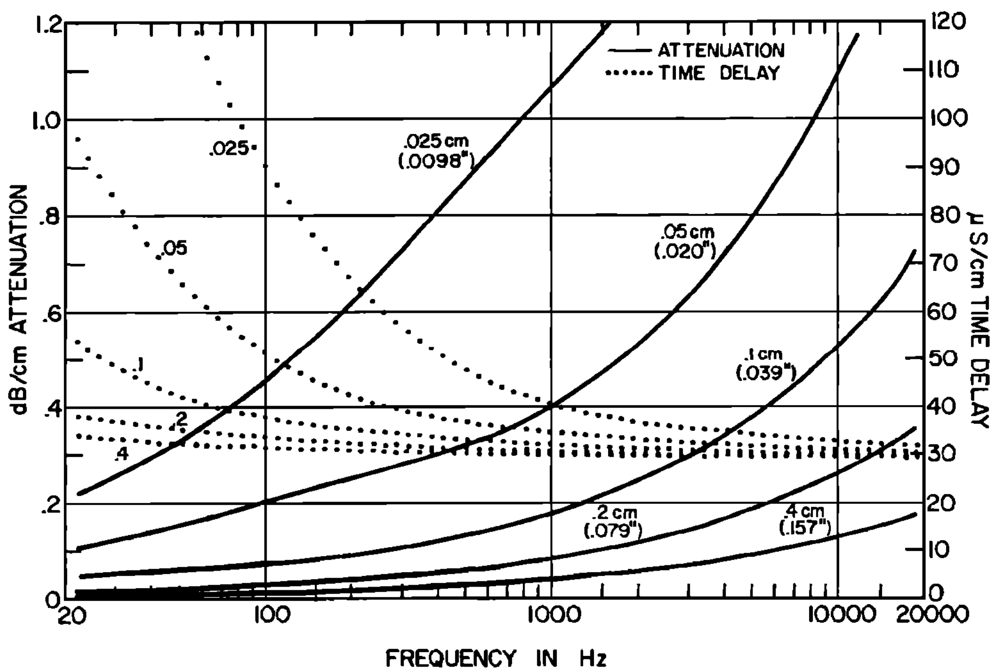

FIG. 11. Attenuation and time delay of a circular tube with diameter as parameter calculated using the full Bessel-function solution.

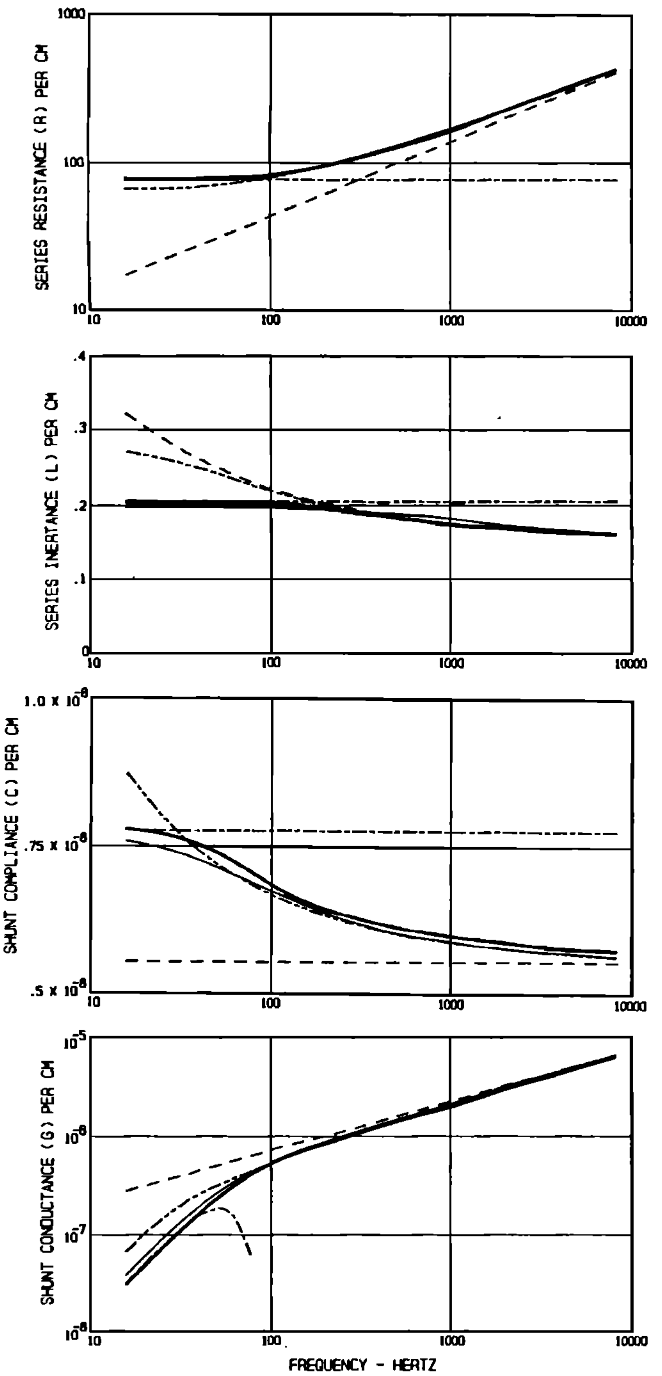

FIG. 12. Per unit-length cgs acoustical series resistance in ohms (a), series inertance in henries (b), shunt compliance in farads (c), and shunt conductance in mhos (d), calculated for a 1-mm-i.d. tube ($a = 0.05$ cm) using several approaches:—: Full Bessell-function solution, —: Present approximation,– – –: Flanagan,[1]– - –: Keefe,[8] small R, – - - -: Keefe,[8] large R.

for air having thermal conductivity KAPPA and specific heat CP.

Finally, the Bessel integrals are given by

$$JN(Z) = \left(\frac{1}{\mathrm{PI}}\right) * \int_0^{\mathrm{PI}} \cos[Z * \sin(x) - N * x] dx, \tag{18}$$

where Z is the complex argument and N is the order of the Bessel function of the first kind.[11]

B. Calculated tube data

Figure 8 shows a plot of the real and imaginary parts of the shunt admittance per unit-length of an acoustic tube, calculated with sufficient terms in the integral representation of the Bessel functions to ensure 0.1% accuracy. The admittance is plotted for convenience in terms of the shunt compliance (parallel circuit representation) $C = YT/(J * W)$ that has been normalized by dividing by the equivalent compliance a tube of that volume would exhibit per unit length if only isothermal compression occurred. Thus the (complex) quantity plotted in Fig. 7 is $CN = C/(V0/P0)$.

Figure 9 shows the normalized series impedance per unit length (real and imaginary parts) obtained from the same Bessel solution. In this case, the normalization is conveniently realized by dividing the series impedance by RHO/(PI*RADIUS**4) (high-frequency inertance divided by the radius squared). These novel normalizations were chosen to provide "universal" plots of the exact Bessel-function solution, an advantage we felt outweighed the unintuitive nature of the normalizations themselves.

The functions in Figs. 8 and 9 undergo a transition near W*RADIUS**2 = 1, although it should be noted that asymptotic values are not realized even for frequencies that are two or three orders of magnitude away from this "transition" frequency.

C. Circuit parameters

The characteristic impedance $Z0$ of a tube expresses the impedance one would see into an infinitely long tube of constant diameter. The Bessel solutions for the real and imaginary parts of $Z0$ as a function of frequency, calculated according to Eq. (3) for various tube diameters, are plotted in Fig. 10.

The propagation constant GAMMA expresses the per unit-length attenuation in Np/cm (1 Np = 8.686 dB) and phase shift in rad/cm. Those values, calculated according to Eq. (4) using the Bessel solution, are shown in Fig. 11.

III. COMPARISON TO OTHER RECENT APPROXIMATIONS

Figures 2–9 of Benade's article[11] are a presentation of what is ostensibly the same data as given here in Figs. 8–11. Although we have chosen a somewhat different normalization procedure, the results are (much to our satisfaction) nearly identical.

White *et al.*[27] showed good agreement, for tubes of 1-, 2-, and 7.48-mm internal diameter, between calculations based on Flanagan's[1] approximations and a more exact solution they derived based on similar assumptions. At the suggestion of one of the reviewers, we are including a comparison between Flanagan's[1] approximations, our approximations, and the Bessel-function solution. For this purpose, we assumed a 1-mm-i.d. tube, one of the diameters for which the White *et al.* comparison was available. (We believe the ordinate in Fig. 11 in White *et al.* is mislabeled and should be in units of 10^{-4} mhos rather than 10^{-3} mhos, incidentally.[28]) This comparison is shown in Fig. 12. For the small tubes of primary interest to us, it appears that the present approximations are more appropriate. This conclusion is supported by the experimental findings described earlier.

Also shown in Fig. 12 is a comparison of Keefe's[8] "small R" and "large R" approximations that, as expected, agree quite well with the full Bessel-function solution in their respective regions of applicability but not as well in the transition region. [In a recent verbal communication, Keefe confirmed our belief that his Eq. (11b) (Ref. 8) has an a^4 term that should be an a^2 term, and his Eq. (11c) has an a^2 term that should be an a^4 term. The comparisons in Fig. 12 were made using these corrections, which yield the correct physical units for inductance and conductance per unit length and eliminate a two-order-of-magnitude discrepancy in the calculated values.]

The constants used for all comparisons (for air at 21 °C and a barometric pressure of 760 mm Hg) are given as follows:

$$U = 0.000\,184 \text{ dyn s cm}^{-2},$$

$$\text{RHO} = 0.0012 \text{ g cm}^{-3},$$

$$C = 34400 \text{ cm s}^{-1},$$

$$P0 = 1\,001\,600 \text{ dyn cm}^{-2},$$

$$\text{KAPPA} = 0.000\,61 \text{ cal s}^{-1}\,{}^\circ\text{C}^{-1}\,\text{g}^{-1},$$

$$CP = 0.24 \text{ cal}\,{}^\circ\text{C}^{-1}\,\text{g}^{-1}.$$

A similar set of self-consistent values for these constants, along with their temperature coefficients, is given in Table II of Benade's[10] article, to which the reader is referred.

ACKNOWLEDGMENTS

We wish to thank Dr. Hugh Knowles, the founder of Industrial Research Products, Inc., for supporting this research. Much of the careful experimental work was performed by Edward Monser.

[1] J. L. Flanagan, *Speech Analysis Synthesis and Perception* (Springer-Verlag, Berlin, 1972), 2nd ed., pp. 25–35.

[2] In FORTRAN, variables $Z0$, $Z1$, $Z2$, GAMMA, $P1$, $P2$, ZT, and YT must be defined as complex numbers. Also, variables starting with letters I–N (LENGTH, $M1$–$M4$, etc.) must be defined as real to avoid the FORTRAN default designations of such variables as integers.

[3] H. L. F. Helmholtz, "On the Influence of Friction in the Air on Sound Motion," Verh. Natur. Histor. Medizin. Ver. Heidelberg III, 16 (1863).

[4] G. R. Kirchhoff, "On the Influence of Thermal Conduction in a Gas on the Motion of Sound," Poggendorfer Ann. **134**, 177–193 (1868).

[5] A. S. Iberall, "Attenuation of Oscillatory Pressures in Instrument Lines," J. Res. Natl. Bur. Stand. **45**, 85–108 (1950).

[6] C. Zwikker and C. W. Kosten, *Sound Absorbing Materials* (Elsevier, New York, 1949), pp. 25–51.

[7] H. F. Olson, *Acoustical Engineering* (Von Nostrand, New York, 1957), p. 89.

[8] D. H. Keefe, "Acoustical Wave Propagation in Cylindrical Ducts: Transmission Line Parameter Approximations for Isothermal and Nonisothermal Boundary Conditions," J. Acoust. Soc. Am. **75**, 58–62 (1984).

[9] *Note added in proof:* Only the numeric value of WN, stripped of its physical dimensions ($\text{s}^{-1}\,\text{cm}^2$), is used in calculating factors M1–M4.

[10] T. F. Hueter and R. H. Bolt, *Sonics* (Wiley, New York, 1955), pp. 406–416.

[11] A. H. Benade, "On the Propagation of Sound Waves in a Cylindrical Conduit," J. Acoust. Soc. Am. **44**, 161–623 (1968).

[12] E. Jahnke and F. Emde, *Tables of Functions* (Dover, New York, 1945), p. 150.

[13] H. Lamb, *The Dynamical Theory of Sound* (Dover, New York, 1960), p. 198.

[14] P. M. Morse and K. U. Ingard, *Theoretical Acoustics* (McGraw-Hill, New York, 1968), pp. 270–294.

[15] M. J. E. Golay, "Theoretical Consideration in Heat and Infra-Red Detection, with Particular Reference to the Pneumatic Detector," Rev. Sci. Instrum. **18**, 353 (1947).

[16] F. B. Daniels, "Acoustical Impedance of Enclosures," J. Acoust. Soc. Am. **19**, 569–571 (1947).

[17] F. Biagi and R. K. Cook, "Acoustical Impedance of a Right Circular Cylindrical Enclosure," J. Acoust. Soc. Am. **26**, 506–509 (1954).

[18] P. V. Bruel, "The Accuracy of Condenser Microphone Calibration Methods," Bruel & Kjaer (Copenhagen) Tech. Rev. **4**, 19–20 (1964).

[19] I. B. Crandall, *Theory of Vibrating Systems and Sound* (Von Nostrand, New York, 1927), pp. 229–237.

[20] E. V. Carlson and M. C. Killion, "Subminiature Directional Microphones," J. Audio Eng. Soc. **22** (2), 92–96 (1974).

[21] G. W. Stewart and R. B. Lindsay, *Acoustics* (Von Nostrand, New York, 1957), p. 89.

[22] D. P. Egolf, "Mathematical Modeling of a Probe-Tube Microphone," J. Acoust. Soc. Am. **61**, 200–205 (1977).

[23] H. Tijdman, "On the Propagation of Sound Waves in Cylindrical Tubes," J Sound Vib. **39** (1), 1–33 (1975).

[24] L. Beranek, *Noise and Vibration Control* (McGraw-Hill, New York, 1971), p. 214; L. Beranek, *Acoustics* (McGraw-Hill, New York, 1954), pp. 135–137.

[25] L. E. Kinsler and A. R. Frey, *Fundamentals of Acoustics* (Wiley, New York, 1982), 3rd ed., pp. 233–234.

[26] N. Kundt, "Letter from Kundt to Poggendorfer Concerning the Apparent Speed of Sound in Tubes," Monatsber. Dtsch. Akad. Wiss. Berlin (19 Dec. 1867).

[27] R. E. C. White, G. A. Studebaker, H. Levitt, and D. Mook, "The Application of Modeling Techniques to the Study of Hearing Aid Acoustic Systems," in *Acoustic Factors Affecting Hearing Aid Performance*, edited by G. A. Studebaker and I. Hochberg (University Park, Baltimore, MD, 1980).

[28] *Note added in proof:* An acoustical mho, like the electrical siemens (the authors regret the death of the electrical mho), is an inverse ohm.